Neuron
Article

Ephrin-B1 Controls the Columnar Distribution of Cortical Pyramidal Neurons by Restricting Their Tangential Migration

Jordane Dimidschstein,[1] Lara Passante,[1] Audrey Dufour,[1] Jelle van den Ameele,[1,7] Luca Tiberi,[1] Tatyana Hrechdakian,[1] Ralf Adams,[3] Rüdiger Klein,[4] Dieter Chichung Lie,[5] Yves Jossin,[6] and Pierre Vanderhaeghen[1,2,*]
[1]Université Libre de Bruxelles (ULB), Institute for Interdisciplinary Research (IRIBHM), and ULB Institute of Neuroscience (UNI), 808 Route de Lennik, B-1070 Brussels, Belgium
[2]Welbio, Université Libre de Bruxelles (ULB), 808 Route de Lennik, Brussels B-1070, Belgium
[3]Department of Tissue Morphogenesis, Max Planck Institute for Molecular Biomedicine, Röntgenstraße 20, Muenster 48149, Germany; and Medical Faculty of Muenster, University of Muenster, Domagkstraße 3, Muenster 48149, Germany
[4]Department of Molecular Neurobiology, Max Planck Institute of Neurobiology, Am Klopferspitz 18, Munich-Martinsried 82152, Germany
[5]Institute of Biochemistry, Emil Fischer Center, University of Erlangen-Nuremberg, Schuhstraße 19, Erlangen 91052, Germany
[6]Division of Basic Sciences, Fred Hutchinson Cancer Research Center, 1100 Fairview Avenue North, Seattle, WA 98109, USA
[7]Department of Neurology, Faculty of Medicine and Health Sciences, Ghent University Hospital, Ghent B-9000, Belgium
*Correspondence: pierre.vanderhaeghen@ulb.ac.be
http://dx.doi.org/10.1016/j.neuron.2013.07.015

SUMMARY

Neurons of the cerebral cortex are organized in layers and columns. Unlike laminar patterning, the mechanisms underlying columnar organization remain largely unexplored. Here, we show that ephrin-B1 plays a key role in this process through the control of nonradial steps of migration of pyramidal neurons. In vivo gain of function of ephrin-B1 resulted in a reduction of tangential motility of pyramidal neurons, leading to abnormal neuronal clustering. Conversely, following genetic disruption of ephrin-B1, cortical neurons displayed a wider lateral dispersion, resulting in enlarged ontogenic columns. Dynamic analyses revealed that ephrin-B1 controls the lateral spread of pyramidal neurons by limiting neurite extension and tangential migration during the multipolar phase. Furthermore, we identified P-Rex1, a guanine-exchange factor for Rac3, as a downstream ephrin-B1 effector required to control migration during the multipolar phase. Our results demonstrate that ephrin-B1 inhibits nonradial migration of pyramidal neurons, thereby controlling the pattern of cortical columns.

INTRODUCTION

During development of the cerebral cortex, pyramidal neurons migrate along the radial glia scaffold toward their final position to complete maturation and establish functional networks (Kriegstein and Noctor, 2004; Marín and Rubenstein, 2003; Rakic, 1988). Cortical radial glia progenitors and their neuronal progeny are thus arranged radially, constituting ontogenic columns of sister neurons; however, it is interesting to note that migrating pyramidal neurons also undergo limited but significant lateral/tangential dispersion (Noctor et al., 2004; Tabata and Nakajima, 2003; Tan and Breen, 1993). This may have a direct impact on the structural and functional organization of cortical columns, since sister neurons derived from the same progenitor display selective patterns of connectivity with each other and/or share similar functional properties (Li et al., 2012; Ohtsuki et al., 2012; Yu et al., 2009, 2012). However, very little is known about the mechanisms of the tangential spread of pyramidal neurons, in contrast with expanding knowledge on radial migration (Bielas et al., 2004; Kriegstein and Noctor, 2004; Marín and Rubenstein, 2003; Marín et al., 2010).

Time-lapse analyses have revealed that migrating pyramidal neurons pass through several transitions on their way to the cortex, including nonradial phases of migration (Noctor et al., 2004; Tabata and Nakajima, 2003). After a short radial migration toward the subventricular zone (SVZ), the immature neurons transiently adopt a multipolar morphology, characterized by dynamic cell processes and the ability to spread tangentially, before adopting again a bipolar morphology and resuming strictly radial migration toward the cortical plate (CP). Several genes have been shown to control the transition between multipolar to bipolar stages with direct consequences on patterns of radial migration (Friocourt et al., 2008; Fuentes et al., 2012; Guerrier et al., 2009; Ip et al., 2011; Jossin and Cooper, 2011; LoTurco and Bai, 2006; Ohshima et al., 2007; Pacary et al., 2011; Pinheiro et al., 2011; Sun et al., 2010; Uchino et al., 2010; Westerlund et al., 2011), but their effect on tangential spread remains poorly known.

Ephrin guidance factors and their Eph receptors are involved in many developmental and homeostatic neural processes, from neurogenesis to axon guidance and synaptic plasticity (Clandinin and Feldheim, 2009; Egea and Klein, 2007; Genander and Frisén, 2010; Klein, 2009). They are divided into two main subfamilies of ligand/receptor couples, ephrin-A/EphA and ephrin-B/EphB, based on their specific structure and binding affinities (Flanagan and Vanderhaeghen, 1998). In many cases, ephrins act as classical ligands for Ephs to initiate a so-called forward signaling, but they can also act as receptors for Ephs through a process of reverse signaling, thus enabling bidirectional cell-to-cell

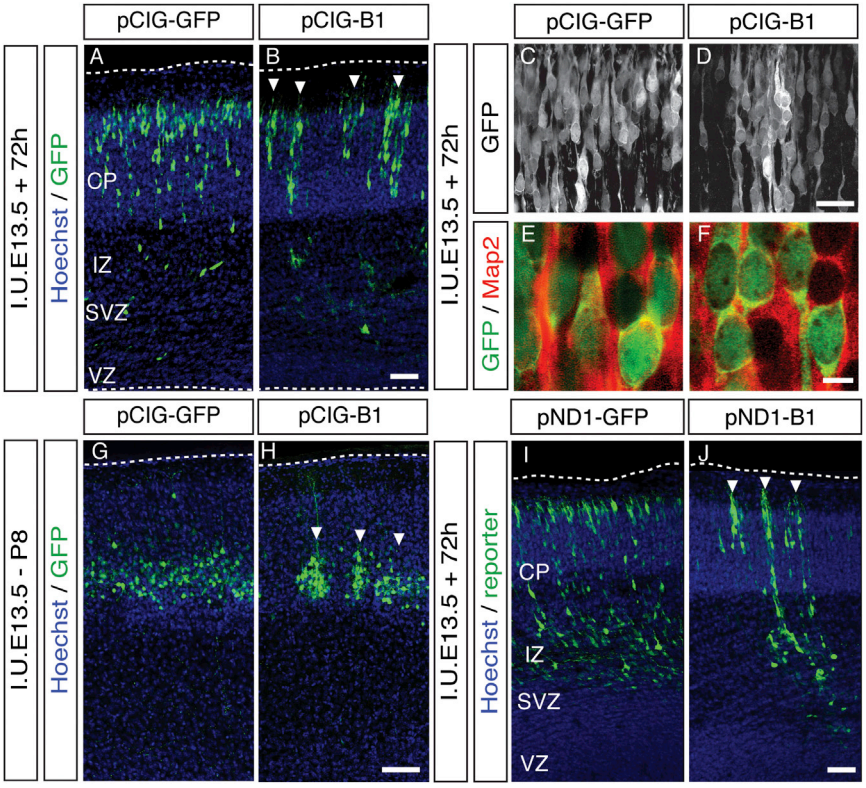

Figure 1. Ephrin-B1 Overexpression Disrupts Lateral but Not Radial Distribution of Pyramidal Neurons in the CP

(A–J) Mouse embryos were electroporated in utero at E13.5, with plasmids expressing GFP [shown in (A), (C), (E), (G), and (I)] or ephrin-B1-IRES-GFP [shown in (B), (D), (F), (H), and (J)] under the control of a ubiquitous CAG promoter [in (A) through (H)] or the neuronal-specific NeuroD1 promoter [in (I) and (J)] and analyzed after 72 hr [in (A) through (F), (I), and (J)] or at postnatal day 8 [in (G) and (H)]. Morphology of electroporated cells within the CP is shown in (C) and (D). (E) and (F) show the immunostaining of electroporated cells for GFP (in green) and Map2 (in red) of the cells following overexpression of GFP (E) or ephrin-B1 (F). Mouse embryos were electroporated in utero at E13.5, with plasmids expressing GFP (G) or ephrin-B1-IRES-GFP (H) under the control of a ubiquitous promoter and analyzed at postnatal day 8 (P8). In (I) and (J), mouse embryos were electroporated in utero at E13.5, with plasmids expressing GFP (G) or ephrin-B1-IRES-GFP (H) under the control of a neuron-specific promoter (NeuroD) and analyzed after 72 hr. Arrowheads indicate the clusters of neurons, and dotted lines indicate the basal surface of the cortex.

Scale bars, 100 μm (G and H); 50 μm (A, B, I, and J); 25 μm (C and D); and 5 μm (E and F). See also Figures S1 and S2.

communication (Batlle and Wilkinson, 2012; Egea and Klein, 2007; Klein, 2009). Recently, ephrin-A/EphA forward signaling was shown to control the lateral distribution of pyramidal neurons by promoting their tangential intermingling during migration (Torii et al., 2009), but the underlying mechanisms remain unclear. Ephrin-Bs were proposed recently to modulate cortical progenitor differentiation and apical adhesion (Arvanitis et al., 2013; Qiu et al., 2008), reelin signaling (Sentürk et al., 2011), and migration of Cajal-Retzius neurons (Villar-Cerviño et al., 2013).

Here, we investigated the role of ephrin-B1 in cortical neuron migration. Using in vivo gain and loss of function, combined with time-lapse analyses, we demonstrate that ephrin-B1 reverse signaling is a key regulator of the lateral distribution of pyramidal neurons. Ephrin-B1 specifically inhibits neurite dynamics and restricts tangential migration of pyramidal neurons during their multipolar phase without impacting on radial migration patterns. Furthermore, we identified the P-Rex1 guanine exchange factor (GEF) for Rac3 as a key effector required downstream of ephrin-B1 in this process. These data shed light on the molecular and cellular mechanisms underlying an important but overlooked aspect of cortical patterning, by providing a link between early migration events and late cortical column organization.

RESULTS

Ephrin-B1 Gain of Function in Pyramidal Neurons Disrupts Their Lateral, but Not Their Radial, Distribution

Ephrin-B1 was previously reported to display a dynamic pattern of expression in newly generated migrating neurons (Stuckmann et al., 2001). We confirmed these observations by immunohistochemistry staining of ephrin-B1 on embryonic cortex at E15.5. This revealed strong expression among the radial glia progenitors of the ventricular zone (VZ), lower levels in the early migrating neurons in transit through the SVZ and intermediate zone (IZ), and weak to absent expression in postmigratory neurons in the CP. No significant immunostaining was observed in ephrin-B1 knockout (KO) mice (Compagni et al., 2003), confirming the specificity of our findings (Figures S1A–S1Eavailable online).

We first examined the role of ephrin-B1 in neuronal migration by gain of function, using mouse in utero electroporation at mid-corticogenesis. This revealed a striking alteration of the lateral distribution of electroporated cells, resulting in the formation of compact clusters following their migration in the CP, which contrasted with the homogeneous distribution observed in control conditions (Figures 1A and 1B). The clusters consisted of pyramidal neurons, assessed by expression of the neuronal marker Map2, and a typical bipolar morphology (Figures 1C–1F). Of note, this effect on clustered lateral distribution was still observed 2 weeks later (in P8 animals) (Figures 1G and 1H). Despite these marked effects, the laminar distribution of the neurons was comparable between ephrin-B1 gain-of-function and control conditions, indicating that only the tangential, but not the radial, distribution of the neurons was altered (Figures 1G and 1H; Figure S2B).

To determine whether the effect on lateral distribution of pyramidal neurons resulted from overexpression in neurons rather than in the radial glial cell scaffold, ephrin-B1 was overexpressed

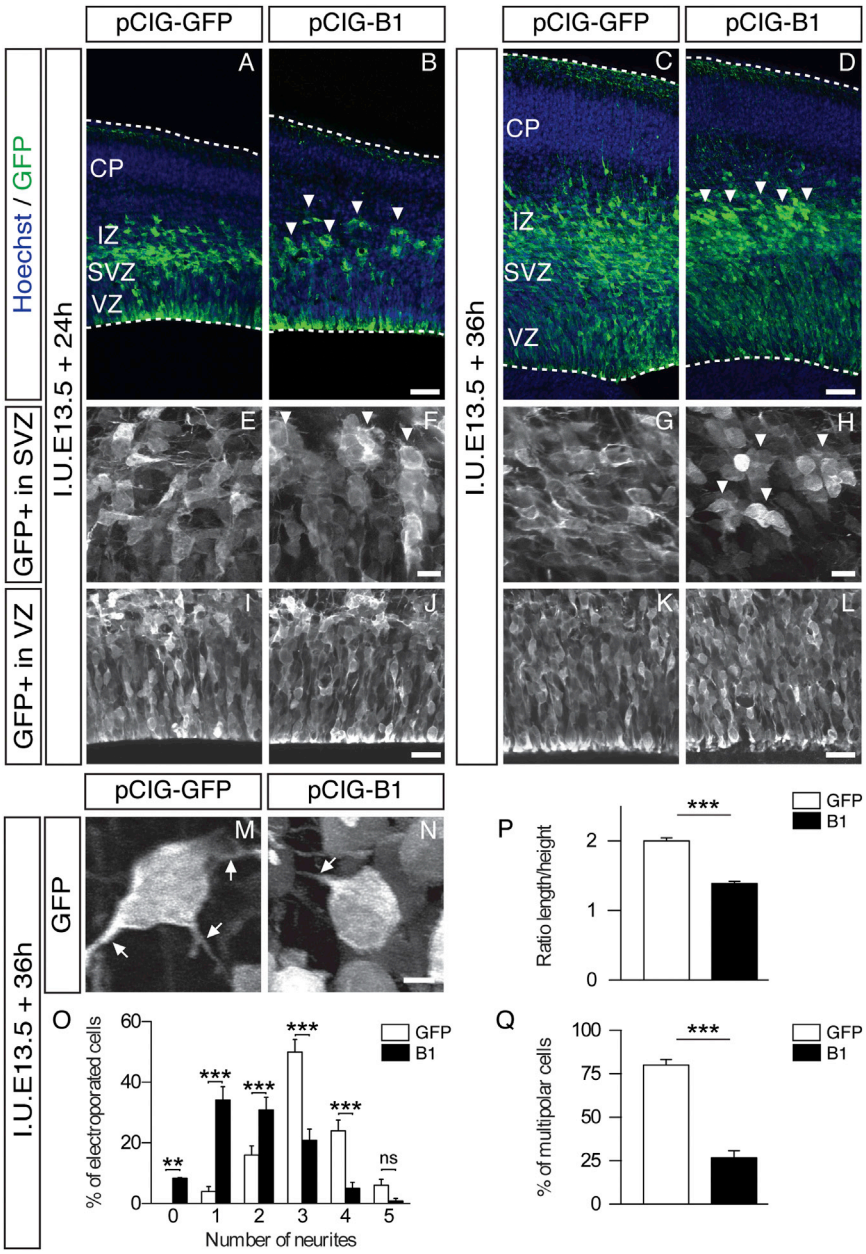

Figure 2. Ephrin-B1 Overexpression Disrupts Lateral Distribution and Morphology of Migrating Neurons at the Multipolar Stage

(A–N) Mouse embryos were electroporated in utero at E13.5 with plasmids expressing GFP [in (A), (C), (E), (G), (I), (K), and (M)] or ephrin-B1-IRES-GFP [in (B), (D), (F), (H), (J), (L), and (N)] and analyzed after 24 hr [in (A), (B), (E), (F), (I), and (J)] or 36 hr [in (C), (D), (G), (H), (K), and (L)]. (E-L) show morphology of electroporated cells within the SVZ in (E) through (H) and the VZ in (I) through (L). In (M) and (N), high magnification of GFP+ multipolar neurons within the SVZ following overexpression of GFP (M) or ephrin-B1 (N).

(O) Proportion of GFP+ cells with the indicated number of neurites within the SVZ.

(P) Ratio of length/height of the GFP+ cells within the SVZ as an indicator of cell shape.

(Q) Percentage of GFP+ neurons with more than two neurites within the SVZ. For GFP, n = 150 in five embryos; for ephrin-B1, n = 120 in four embryos in (O) through (Q). Arrowheads indicate the clusters of neurons, arrows indicate the neurites, and dotted lines indicate the limits of the cortex. Scale bars, 50 μm (A–D), 25 μm (I–L), 10 μm (E–H), and 5 μm (M and N). Bar graphs are plotted as mean ± SEM. In (O), a two-way ANOVA on raw data was conducted, followed by a Tukey's post hoc test. In (P), a Mann-Whitney rank sum test was conducted. In (Q), a z test was conducted. ns, nonsignificant. $^{**}p < 0.01$. $^{***}p < 0.001$.

selectively in migrating neurons by using the NeuroD1 promoter (Hand et al., 2005). This revealed a similar alteration of the lateral distribution of the electroporated neurons (Figures 1I and 1J), indicating that selective gain of function in postmitotic neurons is sufficient to induce the formation of the clusters.

Ephrin-B1 Disrupts the Distribution and Morphology of Migrating Neurons at the Multipolar Stage

These results indicate that ephrin-B1 perturbs robustly the lateral distribution of migrating pyramidal neurons, but what could be the underlying cellular mechanism? The clustering of the neurons could be due to increased adhesion between each other. To test for this possibility, we determined directly the adhesive properties of ephrin-B1 overexpressing pyramidal neurons (obtained by in utero electroporation) dissociated on substrates coated with recombinant ephrin-B1 or ephrin-B1-interacting Eph receptor (EphB2). This revealed that ephrin-B1-expressing neurons tended to adhere less to their substrate compared to green fluorescent protein (GFP)-electroporated neurons, and no increased adhesion could be observed on ephrin-B1- or EphB2-coated substrates (Figure S2A). In addition, examination of the adherent cell distribution revealed no increased aggregation in ephrin-B1-expressing neurons (data not shown). Overall, these data suggest that the clustering observed in vivo cannot be easily explained by direct homoadhesion or proadhesive effects of ephrin-B1-Eph interactions.

We next examined neuronal migration in more detail, by analyzing the effects of ephrin-B1 gain of function after shorter time periods (24–36 hr). Examination of the ephrin-B1-electroporated cells in the VZ revealed a homogeneous distribution of transfected cells at either time point examined (Figures 2A–2D and 2I–2L), suggesting that the first phase of radial migration from the VZ to the SVZ is not affected. In contrast, the neurons that had reached the SVZ/IZ displayed tangential clustering, already after 24 hr, and even more after 36 hr following

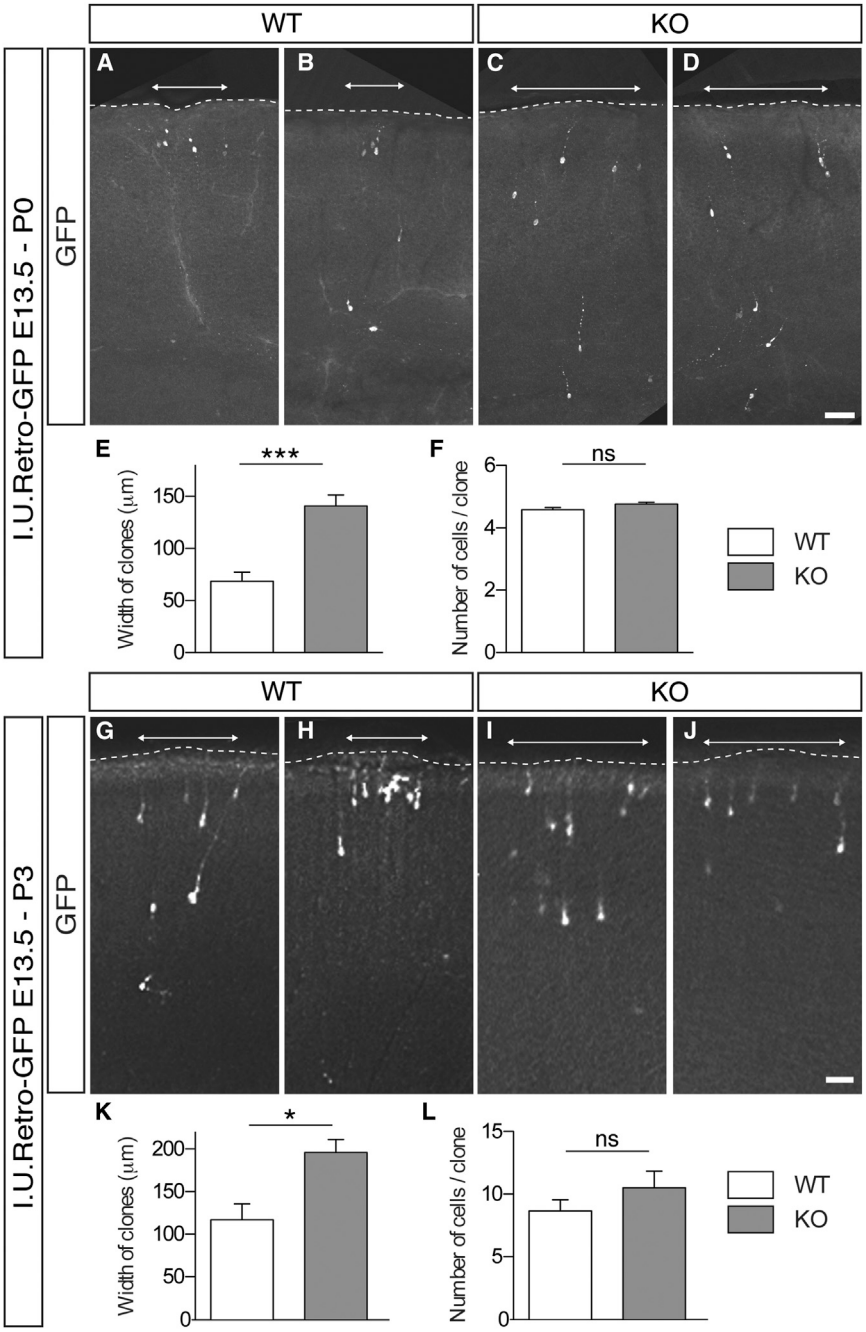

Figure 3. Ephrin-B1 Loss of Function Disrupts the Lateral Dispersion of Ontogenic Cortical Columns in the CP

(A–L) Ephrin-B1 WT [in (A), (B), (G), and (H)] and KO (C), (D), (I), and (J)] mouse embryos were injected in utero at E13.5 with retrovirus expressing GFP, immunostained for GFP, and analyzed at P0 [in (A) through (F)] or P3 [in (G) through (L)]. In (E) and (K), cortical clones were defined as isolated groups of radially oriented GFP+ neurons in the somatosensory cortex. Width of cortical clones measured at the pial surface: P0-WT, n = 19 clones in seven embryos; P0-KO, n = 25 clones in six embryos; P3-WT, n = three clones in two embryos; P3-KO, n = six clones in three embryos). (F) and (L) show the number of cells per clone (P0-WT, n = 87 cells in 19 clones; P0-KO, n = 119 cells in 25 clones; P3-WT, n = 26 cells in three clones; P3-KO, n = 63 cells in six clones).

Dotted lines indicate the limits of the cortex, and double arrows represent the lateral limits of cortical clones. Bar graphs are plotted as mean ± SEM. Scale bars, 50 μm (A– D) and 100 μm (G–J). In (E), (F), (K), and (L), a Student's t test was used. ns, nonsignificant. *$p < 0.05$. ***$p < 0.001$. See also Figures S3 and S4.

electroporation (Figures 2A–2H). It is intriguing that the neurons within SVZ/IZ appeared with an altered morphology, characterized by a rounder shape and a reduction in the number of neurites (Figures 2F, 2H, 2M, and 2N). Indeed, quantification of neuronal morphology in the SVZ/IZ further revealed that ephrin-B1 overexpression resulted in a lower length-to-height ratio, a smaller number of neurites, and a decrease in the proportion of neurons displaying multipolar morphology (Figures 2O–2Q).

Altogether, these data demonstrate that ephrin-B1 transiently affects the morphology of pyramidal neurons, specifically during the phase of multipolarity and tangential migration. This results in the formation of clusters of neurons within the SVZ/IZ by reducing the ability of these neurons to migrate tangentially.

Ephrin-B1 Loss of Function Disrupts the Lateral Dispersion of Ontogenic Cortical Columns

To test for a required function of ephrin-B1 in the migration and positioning of pyramidal neurons, we next examined the effects of a depletion of ephrin-B1 in cortical neurons, using ephrin-B1 KO mice (Compagni et al., 2003). Inspection of brain architecture at embryonic and perinatal stages did not reveal marked defects. The aspect of the radial glia scaffold and the density and thickness of the CP, as well as upper and deep layers (revealed by expression of Cux1 and Ctip2, respectively), were all comparable between wild-type (WT) and KO animals at all inspected levels (Figure S3). Collectively, these results indicate that the radial positioning of pyramidal neurons appears to be largely unaffected in mice depleted for ephrin-B1.

We next analyzed the tangential distribution of pyramidal neurons in ephrin-B1 KO mice, using retrovirus-mediated lineage tracing, enabling to label single clusters of clonally related neurons (Figure 3; Figure S4) (Jessberger et al., 2007; Valiente et al., 2011; Yu et al., 2009). Remarkably, examination of infected

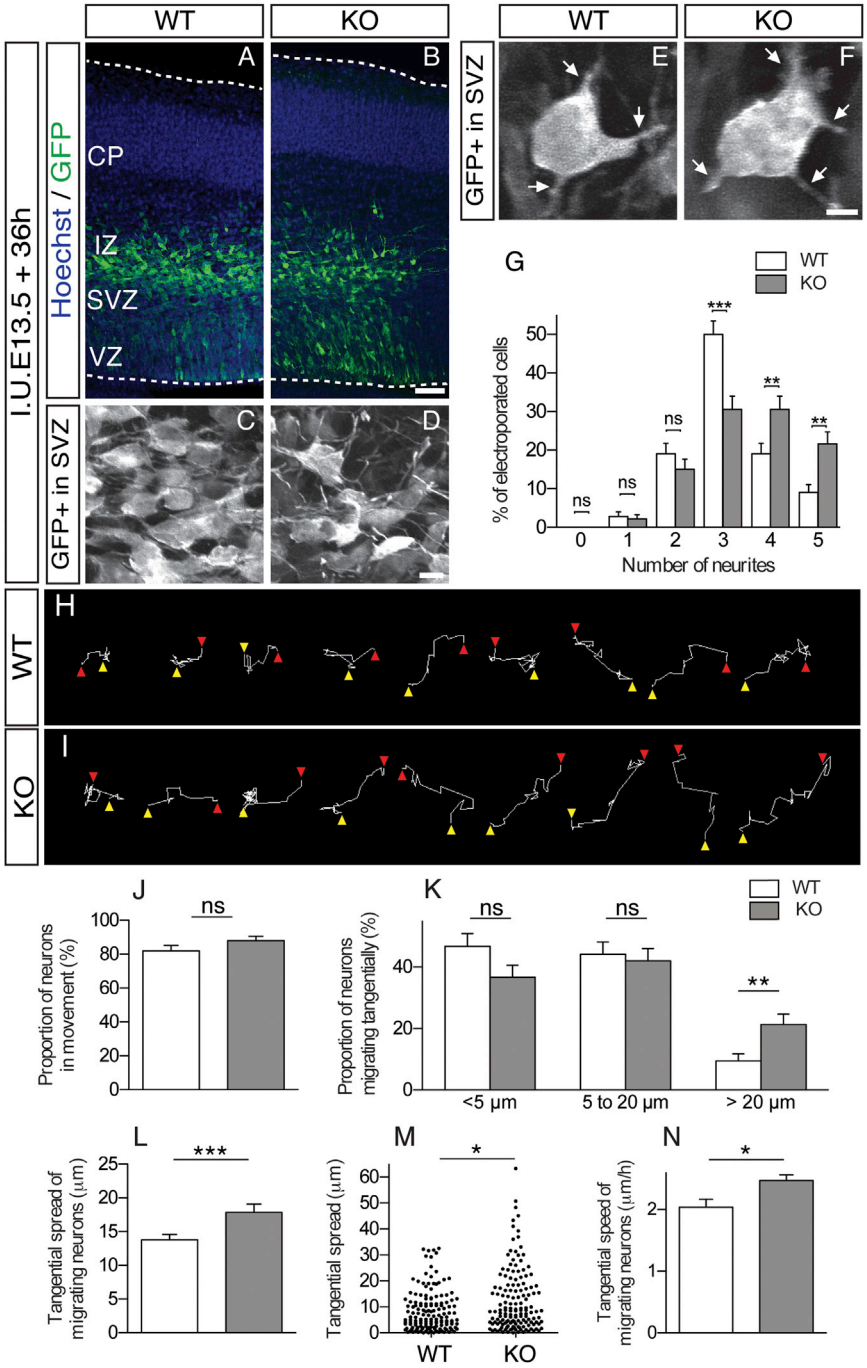

Figure 4. Ephrin-B1 Loss of Function Disrupts the Morphology and Enhances Tangential Migration of Multipolar Cells in the SVZ

(A–G) WT and KO mouse embryos were electroporated in utero at E13.5, with plasmids expressing GFP and analyzed after 36 hr. Dotted lines indicate the limits of the cortex. (A) and (B) show the distribution of GFP+ neurons throughout the cortex. (C) and (D) show morphology of GFP+ neurons within the SVZ. (E) and (F) show high magnification of multipolar neurons within the SVZ, arrows indicate the position of the neurites. (G) shows the proportion of neurons within the SVZ according to the indicated number of neurites. (WT: n = 210 in five embryos; KO: n = 180 in four embryos).

(H–N) Time-lapse analysis of multipolar neurons within the SVZ (n = 150 cells tracked in five movies for five WT and five KO animals). (H) and (I) show representative tracks of migration paths of WT (H) and ephrin-B1 mutant (I) neurons within the SVZ. Yellow and red arrowheads mark the starting point and the endpoint of migration, respectively. (J) shows the percentage of neurons in movement, calculated as the percentage of neurons that migrated more than 5 μm away from their starting position, independent of the orientation. (K) shows the percentage of neurons that spread tangentially less than 5 μm; between 5 and 20 μm; and over 20 μm. (L) shows the average tangential spread of the neurons that migrated at least 5 μm (18.2 ± 1.2 μm in WT; 26.6 ± 1.8 μm in KO). (M) shows the plotted distribution of the tangential spread of all tracked neurons. (N) shows the average speed of the neurons that migrate tangentially (2.0 ± 0.1 μm/hr in WT; 2.5 ± 0.1 μm/ht in KO).

Bar graphs are plotted as mean ± SEM. Scale bars, 50 μm (A and B), 25 μm (C and D), and 5 μm (E and F). In (G), a two-way analysis of variance (ANOVA) on raw data followed by Tukey's post hoc test was conducted. In (J) and (K), a z test was conducted. In (L) through (N), a Mann-Whitney rank sum test was conducted. ns, nonsignificant. *$p < 0.05$. **$p < 0.01$. ***$p < 0.001$. See also Figure S5 and Movies S1 and S2.

neurons at day of birth (P0) and postnatal day 3 (P3) showed that the width of ontogenetic clones was consistently increased in the KO mice compared to the WT controls, while the average number of cells per clone, as well as the typical bipolar morphology of pyramidal neurons, were unchanged in the mutants (Figure 3; data not shown). These data demonstrate that ephrin-B1 loss of function results in an increase of the width of ontogenic cortical columns and that ephrin-B1 is required for the normal spatial arrangement of pyramidal neurons along the tangential, but not the radial, axis.

Ephrin-B1 Loss of Function Alters the Multipolar Morphology and the Tangential Migration Patterns of Pyramidal Neurons

To gain insight into the mechanisms underlying the changes observed in cortical ontogenic columns, we analyzed the morphology and behavior of migrating pyramidal neurons using in utero electroporation of a GFP marker plasmid in ephrin-B1 mutant and WT mice (Figures 4A–4G). Analysis of the morphology revealed a more complex shape of migrating multipolar neurons in the SVZ/IZ in the mutants, with more numerous neurites compared to the WT neurons. These results demonstrate that, following ephrin-B1 loss of function, migrating neurons extend more neurites at the multipolar stage.

Several studies have suggested a functional relationship between the number of neurites and neuronal migration (Guerrier

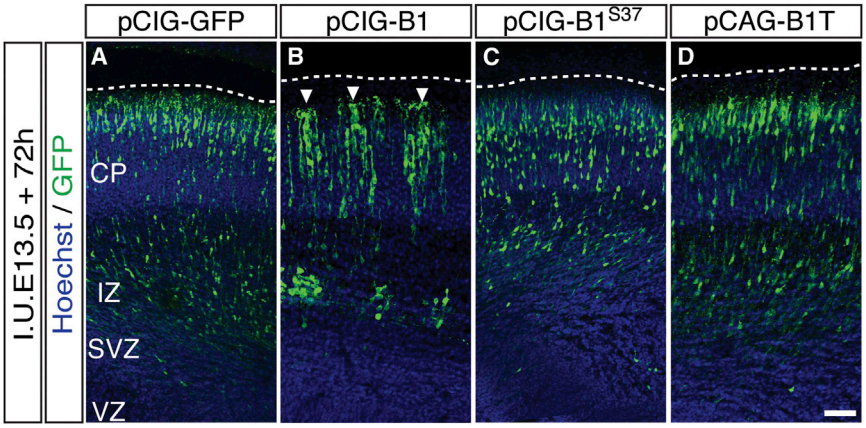

Figure 5. Ephrin-B1 Gain-of-Function Phenotype Depends on Eph-Receptors Interaction and Reverse Signaling

(A–D) Mouse embryos were electroporated in utero at E13.5, with plasmids expressing GFP (A), ephrin-B1-IRES-GFP (B), ephrin-B1^{S37}-IRES-GFP (C), or ephrin-B1T-IRES-GFP (D) and analyzed after 72 hr. Arrowheads indicate the clusters of neurons; dotted lines indicate the pial surface of the cortex. Scale bar represents 50 μm.
See also Figure S6.

et al., 2009; Kwiatkowski et al., 2007). Therefore, we next examined the migration of multipolar neurons in ephrin-B1 mutants, using time-lapse analyses. Following in utero electroporation of GFP marker plasmids, we tracked the neuronal movement in E14.5 organotypic slice cultures, focusing on multipolar neurons in the SVZ/IZ (Figure 4H–4N). A similar proportion of neurons exhibited significant (>5 μm) migratory behavior in the KO animals, compared to WT animals (Figure 4J), but the proportion of neurons migrating extensively (more than 20 μm away from their original position) was significantly increased in ephrin-B1 mutants (Figure 4K). Most strikingly, the mutant neurons displayed wider tangential spread, as well as higher speed (Figures 4H–4N; Movie S1). Of note, the analysis of the migration rate of radially migrating neurons revealed a similar speed of migration between WT and KO (Figure S5A).

To relate these findings to the previous data obtained with ephrin-B1 gain of function, we then performed similar time-lapse analyses following ephrin-B1 gain of function. This revealed that ephrin-B1-overexpressing neurons displayed lower levels of migration and tangential spread (Figures S5C–S5I; Movie S2), thus displaying mirror behavior when compared to the levels of ephrin-B1-deficient neurons. Notably, single and clustered neurons displayed a similarly decreased tangential speed and spread, suggesting that overexpression of ephrin-B1 alters the migration properties of the neurons in the SVZ independently of their proximity with each other (Figures S5G and S5I). Altogether, these results demonstrate that ephrin-B1 is required to control selectively the dynamic morphology and migratory properties of pyramidal neurons during their multipolar transition stage and, thereby, their final tangential spread in the CP.

Ephrin-B1 Control on Tangential Spread of Pyramidal Neurons Requires Eph Receptor Binding and Reverse Signaling

We next examined the molecular mechanisms involved in the selective effects of ephrin-B1 on morphology and migration of pyramidal neurons. It was recently described that ephrin-B1 signaling may be elicited by homointeraction, independently of interaction with EphB receptors (Bochenek et al., 2010). To explore this possibility, we tested by in utero electroporation the effect of a mutated form of ephrin-B1 lacking the ability to interact with EphB receptors (B1^{S37}). Examination of the brains 72 hr after electroporation revealed a homogeneous distribution of the electroporated cells within the CP, comparable to control conditions (Figures 6A–6C). This result indicates that the interaction between ephrin-B1 and Eph receptors is necessary to control the lateral distribution of pyramidal neurons. Immunostaining with antibodies against an epitope common to EphB1/2/3 receptors revealed strong staining throughout the cortical thickness, consistent with previous data on EphB messenger RNA expression, indicating that binding partners of ephrin-B1 neurons can be found among radial glial cells and neurons throughout all cortical compartments (Figure S1B).

Ephrin-B1 can interact with Eph receptors as a ligand or a receptor, through forward and reverse signaling, respectively (Egea and Klein, 2007). To test whether ephrin-B1 reverse signaling was involved, we overexpressed a mutated form of ephrin-B1 where its entire intracellular domain (ephrin-B1T) is replaced by GFP, thereby preventing reverse signaling but preserving targeting to the plasma membrane and binding to Eph receptors (Figure S6). Gain of function of ephrin-B1T revealed a normal, nonclustered, distribution of electroporated cells (Figure 5D), thereby indicating that reverse signaling through the intracellular domain is crucial to induce neuron clusterization on ephrin-B1 gain of function.

Ephrin-B1 Acts through P-Rex1 to Control the Tangential Distribution of Pyramidal Neurons

Ephrin-B reverse signaling has been linked to several regulatory pathways of the cytoskeleton, leading to direct modulation of neurite extension and dynamics, usually through small G proteins (Xu and Henkemeyer, 2009). In order to determine which ephrin-B1-dependent effector(s) may be involved here, we searched for putative intracellular effectors of ephrin-B1 signaling previously identified in functional screens (Huynh-Do et al., 2002; Jørgensen et al., 2009; Xu et al., 2003) and selected those that appeared to be expressed in the cortical SVZ/IZ (according to literature and a search of database websites). We then tested potential candidates functionally using an in vivo targeted "suppressor" screen. Specifically, we performed ephrin-B1 electroporation together with loss-of-function constructs (using dominant-negative forms or RNA interference), looking for suppression of the ephrin-B1-dependent neuronal clustering.

Strong ephrin-B1 clustering effects could still be observed following inhibition of various candidate effectors/pathways, including β-integrins, focal adhesion kinase (FAK), β-2-chimaerin, and Janus kinase (data not shown).

In contrast, the inhibition of P-Rex1, a GEF for Rac (Waters et al., 2008; Yoshizawa et al., 2005) (using a dominant-negative form devoid of GEF domain: Prex1^{DN}) (Yoshizawa et al., 2005), resulted in robust inhibition of ephrin-B1-related clustering (Figures 6A–6O), while the number of cells remained similar in the VZ (Figure S7). No effect was observed following overexpression of WT P-Rex1, confirming the specificity of the inhibition of the dominant-negative form. Moreover, inhibition of P-Rex1 by Prex1^{DN} completely abolished the effect of ephrin-B1 on the morphology of the neurons and number of neurites at the multipolar phase (Figures 6H and 6K). Finally, inhibition of P-Rex1 alone also resulted in an increase of the number of neurites, thus mimicking the effects observed following loss of function of ephrin-B1 (Figures 6I and 6L). Collectively, these data identify P-Rex1 as an important effector of ephrin-B1 in the context of tangential migration of pyramidal neurons.

P-Rex1 is composed of several domains, including a DH domain typical of Rho family GEFs, a PH domain, two DEP domains, two PDZ domains, and a C-terminal half similar to inositol polyphosphate 4-phosphatase (Waters et al., 2008). The presence of the PDZ domains was intriguing, since the C terminus of the intracellular domain of ephrin-B1 contains a PDZ-binding domain. We thus tested for interaction between the two proteins in vivo, first between endogenous ephrin-B1 and exogenous P-Rex1 (which was overexpressed as a tagged protein since we were unable to immunoprecipitate the endogenous P-Rex1 using available antibodies). This revealed a coimmunoprecipitation of the two proteins, which was not detected when using protein extracts of ephrin-B1 KO cortex, confirming the specificity of the interaction (Figure 6P). We next investigated further the nature of ephrin-B1/P-Rex1 interactions. We observed no coimmunoprecipitation between ephrin-B1 and a mutated form of P-Rex1 lacking its PDZ domains (Prex1$^{\Delta PDZ}$) (Figure 6Q). Conversely, a mutated form of ephrin-B1 devoid of its PDZ-binding domain (B1$^{\Delta PDZb}$) could not be coimmunoprecipitated with P-Rex1 (Figure S8).

Altogether, these data suggest that P-Rex1 interacts with ephrin-B1, at least in part, via its PDZ domain.

P-Rex1 was first identified as a GEF activating Rac proteins and recently was shown to act preferentially on Rac3 (Waters et al., 2008). Given that Rac3, contrary to Rac1, was previously shown to decrease the number of neurites and induce cell rounding (Hajdo-Milasinović et al., 2007, 2009), thus reminiscent of the effects of ephrin-B1 observed here, we tested the effect of Rac3 inhibition (using a dominant-negative form, Rac3^{DN}) on ephrin-B1 gain of function. Remarkably, coelectroporation of ephrin-B1 and Rac3^{DN} resulted in complete suppression of the neuronal clustering and neuronal morphology alterations induced by ephrin-B1 alone (Figures 7A–7G). Altogether, these data suggest that ephrin-B1/P-Rex1 act, at least in part, through Rac3 to modulate the morphology and the lateral distribution of pyramidal neurons during the multipolar phase of migration.

DISCUSSION

While the mechanisms regulating radial migration and laminar positioning of pyramidal neurons have become increasingly more established (Bielas et al., 2004; Kriegstein and Noctor, 2004; Marín and Rubenstein, 2003; Marín et al., 2010), much less is known about the control of tangential migration of these cells and how this may affect cortical organization. Our data point to a model whereby ephrin-B1 reverse signaling, acting through the P-Rex1 GEF to activate Rac3, modulates the morphology and tangential migration of pyramidal neurons during their multipolar phase, and this mechanism is required to generate cortical columns with appropriate lateral dispersion (Figure 7H).

Ephrin-As were found recently to control the lateral dispersion of cortical pyramidal neurons (Torii et al., 2009). Specifically, Torii et al. (2009) found a reduction of the lateral dispersion of pyramidal neurons in ephrin-A2/3/5 mutants, together with irregularities in final tangential neuronal layout. By contrast, our results demonstrate that ephrin-B1 loss of function results in increased tangential migration, suggesting that ephrin-A forward and ephrin-B reverse signaling may have opposite effects in the control of tangential migration of pyramidal neurons. Such a complementary effect is reminiscent of how ephrin-A forward and ephrin-B reverse pathways cooperate to control topographic mapping of visual axonal projections (Clandinin and Feldheim, 2009). Somewhat more paradoxically, Torii et al. (2009) also reported that ephrin-A/EphA gain of function resulted in neuronal clustering that is strikingly similar to the one we observed following ephrin-B1 overexpression. While they favor a model where ephrin-A/EphA-mediated clustering results from enhanced migration and tangential intermingling, our refined analyses of the morphology and migration of pyramidal cells strongly suggest an opposite scenario following ephrin-B gain of function. In this case, indeed, cells display a round morphology with very few neurites together with a poor capacity to migrate, leading to their clustering in the SVZ/IZ. As for ephrin-Bs, gain- and loss-of-function phenotypes are thus strictly mirror images in terms of cell properties and final patterning outcome (Figure 7H). It should be noted, however, that the striking clustering observed following ephrin-B1 gain of function could involve, together with the alteration of migratory properties described here, additional effects linked to ephrin overexpression, such as increased cell homoadhesion (Batlle and Wilkinson, 2012), although we did not find evidence for ephrin-B1 proadhesive effects in migrating cortical neurons.

Our dynamic analyses revealed that ephrin-B1 acts mainly during the multipolar phase of migration and that there is a striking correlation between the number/dynamics of neurites displayed by these neurons and their patterns of tangential migration. A key feature of pyramidal neurons during this phase is their exploratory behavior, characterized by dynamic extension and retraction of neurites (Noctor et al., 2004; Tabata and Nakajima, 2003). Several genes have been identified that control specifically the transition between the multipolar phase and subsequent radial migration (Guerrier et al., 2009; Ip et al., 2011; Jossin and Cooper, 2011; LoTurco and Bai, 2006; Ohshima et al., 2007; Pacary et al., 2011; Pinheiro et al., 2011; Westerlund

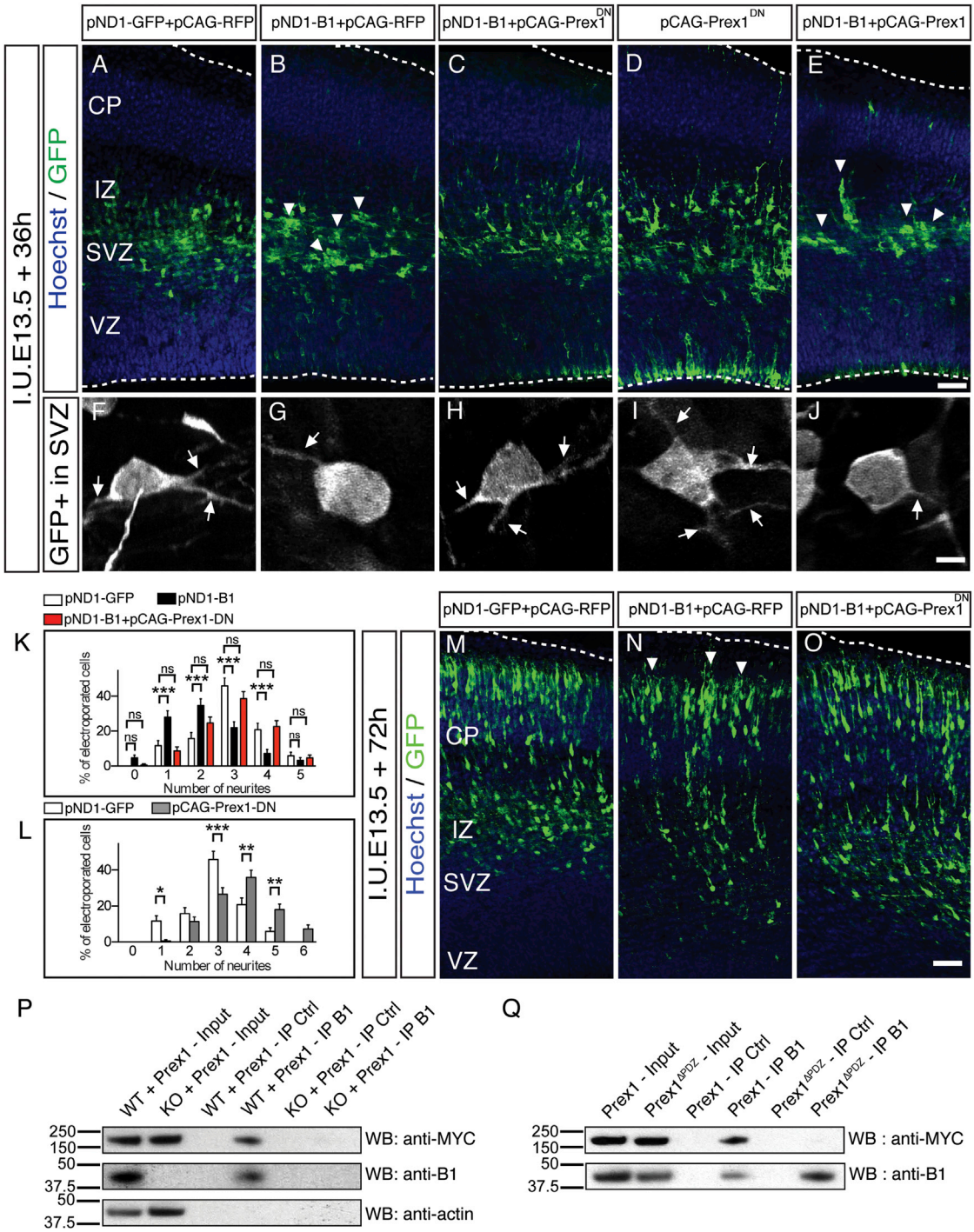

Figure 6. P-Rex1 Modulates the Effect of Ephrin-B1 on the Migration and the Morphology of Migrating Neurons

(A–O) Mouse embryos were electroporated in utero at E13.5 with the indicated plasmids and analyzed after 36 hr [in (A) through (L)] or 72 hr [in (M) through (O)]. In (F) through (J), high magnification of representative multipolar neurons within the SVZ is shown. (K) and (L) show the proportion of GFP+ cells with the indicated number of neurites within the SVZ (n = at least 150 cells in five embryos for each condition). Arrowheads indicate the clusters of neurons, arrows indicate the neurites, and dotted lines indicate the limits of the cortex. Scale bars, 50 μm in (A–E) and (M–O), and 5 μm (F–J). Bar graphs are plotted as mean ± SEM. ***$p < 0.001$. **$p < 0.01$. *$p < 0.05$. In (K) and (L), a two-way ANOVA on raw data was conducted, followed by a Tukey's post hoc test.

(P) E13.5 Ephrin-B1 WT and KO embryos were electroporated with MYC-tagged P-Rex1, and cortex was collected at E14.5. Immunoprecipitation was carried out using control or ephrin-B1 antibody. Total lysate and immunoprecipitates were analyzed by immunoblotting with antibodies directed against ephrin-B1, MYC, or Actin.

(legend continued on next page)

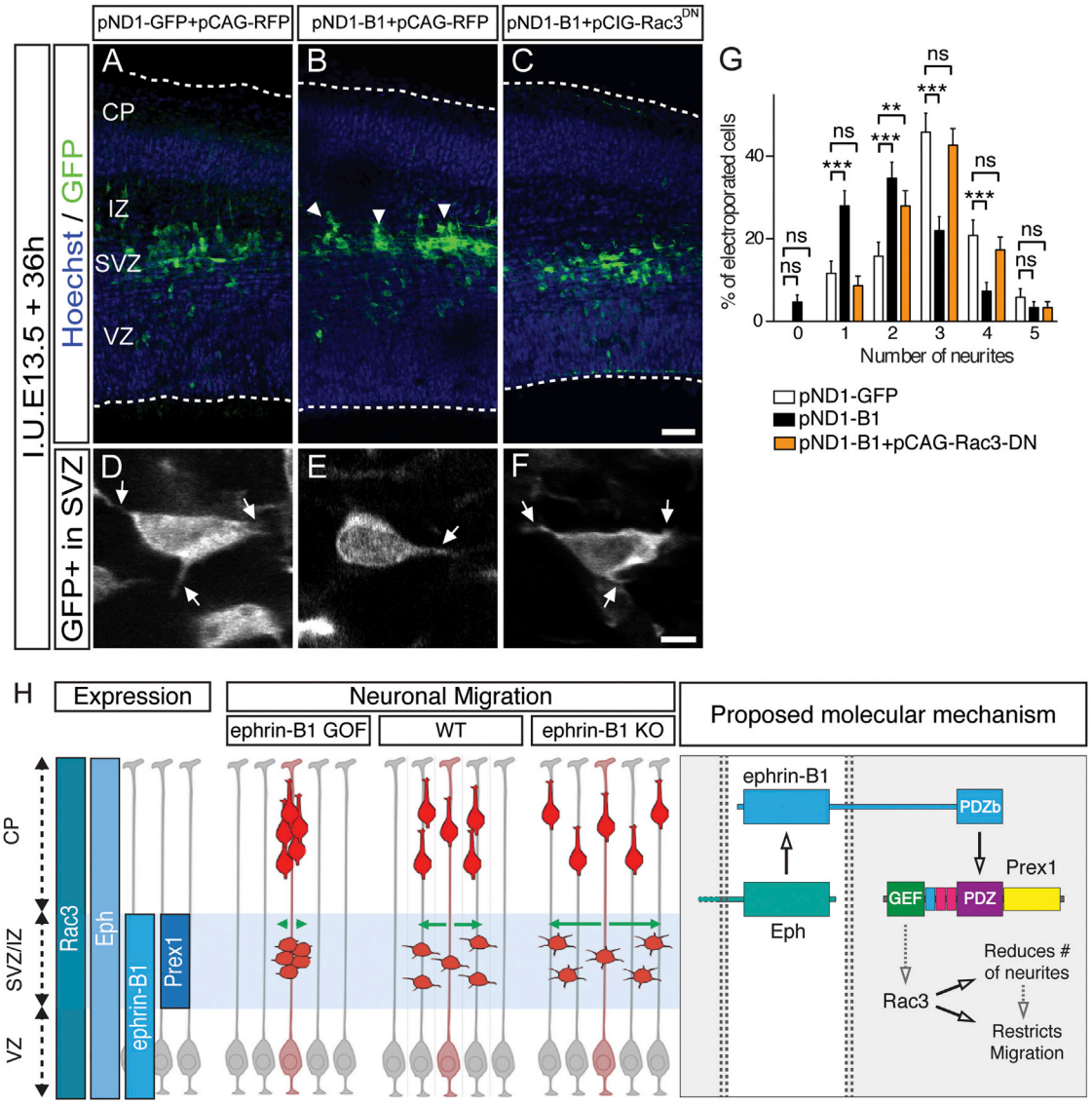

Figure 7. Rac3 Is an Effector of Ephrin-B1

(A–F) Mouse embryos were electroporated in utero at E13.5 with the indicated plasmids and analyzed after 36 hr. (n = at least six animals in three litters for each conditions). (A), (B), and (C) show the distribution of GFP+ neurons throughout the cortex. In (D), (E), and (F), high magnification of representative multipolar neurons within the SVZ is shown. Scale bars, 50 μm (A–C) and 5 μm (F).

(G) shows the proportion of GFP+ cells with the indicated number of neurites within the SVZ (n = at least 150 cells in five embryos for each condition). A two-way ANOVA was conducted on raw data, followed by a Tukey's post hoc test.

(H) Proposed model for ephrin-B1 function during pyramidal neuron migration. See text for further explanations. For P-Rex1 protein, the GEF domain is indicated in green; PH domain, in blue; DEP domains, in pink; PDZ domains, in purple; and Insp-4P domain, in yellow. Arrowheads indicate the clusters of neurons, arrows indicate the neurites, and dotted lines indicate the limits of the cortex. Bar graphs are plotted as mean ± SEM. *$p < 0.05$. **$p < 0.01$. ***$p < 0.001$. ns, nonsignificant.

et al., 2011). In most cases, however, the influence of these genes on patterns of tangential spread and columnar organization remain unexplored, with the notable exception of FAK, which was shown recently to affect the lateral distribution of pyramidal neurons (Valiente et al., 2011). Of note, FAK is known to lie downstream of ephrin-B signaling (Cowan and Henkemeyer, 2001; Jørgensen et al., 2009), but the disruption of FAK did not alter the ability of ephrin-B1 to induce neuronal clustering (data

(Q) E13.5 embryos were electroporated with MYC-tagged P-Rex1 or MYC-tagged P-Rex1 devoid of its PDZ domain (P-Rex1$^{\Delta PDZ}$), and cortex was collected at E14.5. Immunoprecipitation was carried out using control or ephrin-B1 antibody. Total lysate and immunoprecipitates were analyzed by immunoblotting with antibodies directed against ephrin-B1 or MYC.

See also Figure S7.

not shown). Instead, we identified an interactor of ephrin-B1, P-Rex1, as an effector of ephrin-B1-dependent control of columnar organization of pyramidal neurons. P-Rex1 is a PDZ domain-containing GEF for Rac GTPases (Waters et al., 2008; Yoshizawa et al., 2005). It is interesting that it was found to be expressed mostly in the SVZ/IZ, in migrating pyramidal neurons during the multipolar phase, where it could impact neuronal migration (Yoshizawa et al., 2005). The onset of expression of P-Rex1 during this step may explain how ephrin-B1 only alters the migration properties of neurons in the SVZ/IZ and not in the VZ. Our data also suggest that modulation of Rac3 activity is, at least in part, required for ephrin-B1 effects. This is consistent with preferential activity of P-Rex1 on Rac3 (Waters et al., 2008) and on the effects of Rac3 on inhibition neurite extension and induction of cell rounding (Hajdo-Milasinović et al., 2007, 2009), strikingly similar to those observed here for ephrin-B1. While our data strongly suggest that P-Rex1 and Rac3 activity are required for ephrin-B1 gain of function on pyramidal neuron migration, it is possible that P-Rex1 may well act also through other ways, including the modulation of other GTPases, or even, in part, independently of GEF activity. Similarly, while our data indicate that ephrin-B1 and P-Rex1 can interact in vivo through their PDZ/PDZ-binding domain, they may also be part of larger signaling complexes involving additional scaffolding and signaling proteins. Finally, Rac3 may be activated by other means than P-Rex1 in the same context. Nevertheless, our data point to ephrin-B1/P-Rex1/Rac3 as being the first elements of a pathway controlling tangential spread of pyramidal neurons (Figure 7H). It will be interesting in the future to examine neuronal migration in P-Rex1/Rac3 mutant mice, determine whether they articulate with pathways of radial migration, and determine whether ephrin-B1/P-Rex1/Rac3 also act together in other developmental contexts.

Our data show that ephrin-B1 effects are critically dependent on the capacity to bind to Eph receptors. We found broad expression of ephrin-B1-interacting Eph receptor proteins throughout the embryonic cortex, both in cortical progenitors and neurons, to be consistent with previous in situ hybridization data indicating expression of EphB1 (CP), EphB2/EphB3/EphA4 (VZ/SVZ), and EphB6 (SVZ/IZ) (North et al., 2009; Qiu et al., 2008) (http://www.eurexpress.org/ee/). Ephrin-B1-expressing neurons could thus be influenced by Eph receptors displayed by other migrating neurons, and this crosstalk between migrating neurons could lead to the restriction of their tangential dispersion, analogous to the model recently put forward for the spread of cajal-Retzius neurons (Villar-Cerviño et al., 2013), although opposite as for ephrin signaling. Alternatively or in addition, ephrin-B1-expressing neurons could be influenced by Eph receptors displayed on the scaffold of radial glial cells or intermediate progenitors, which could also restrict their tangential migration. The expression profile of many Eph receptors is thus suggestive of their potential implication in the regulation of ephrin-B1, which will be interesting to study in the future, using ad hoc compound mutants for the various ephrin-B1 receptors expressed in migrating pyramidal neurons or radial glial cells.

An interesting observation is that, following these early migration defects, ephrin-B1 mutant mice display abnormal ontogenic cortical columns that are wider at postnatal stages. Of note, cortical ontogenic columns have recently emerged as a key substrate of cortical circuitry, as clonally related neurons establish preferential connectivity with each other and can share similar functional properties (Li et al., 2012; Ohtsuki et al., 2012; Yu et al., 2009, 2012). In this context, ephrin-B1 mutants will constitute an attractive model to study structure-function relationships of these columns, especially since these mutants do not display other overt defects in cortical cytoarchitecture. Indeed, clonally related sister neurons could be less connected in the mutants, because they are more distant from each other. Alternatively, if the connectivity were maintained, the functional radial units would occupy a larger volume, which could modify cortical network function and information processing. Future work involving the detailed analysis of cortical microcircuitry in ephrin-B1 KOs may help address these possibilities and test further the physiological relevance of ontogenic columns.

Altogether, our findings thus shed light on the molecular mechanisms controlling the nonradial patterns of migration of pyramidal neurons and illustrate how alterations of these patterns may affect cortical column architecture and function.

EXPERIMENTAL PROCEDURES

Transgenic Mice, Breeding, and Genotyping

Timed-pregnant mice were obtained from local colonies of mutant and WT mice. The plug date was defined as embryonic day (E)0.5, and the day of birth was defined as P0. Conditional ephrin-B1 KO mice have been described elsewhere (Compagni et al., 2003) and were crossed with mice expressing Cre recombinase under the control of PGK-1 promoter (Lallemand et al., 1998). Animal care and procedures were in compliance with local ethical committees.

In Utero Electroporation

Timed-pregnant mice were anesthesized with a ketamine/xylazine mixture at E13.5, and each uterus was exposed under sterile conditions. Plasmid solutions containing 1 μg/μl of DNA were injected into the lateral ventricles of the embryos using a heat-pulled capillary. Electroporation was performed using tweezers electrodes (Nepa Gene) connected to a BTX830 electroporator (five pulses of 40 V for 100 ms with an interval of 1 s). Embryos were placed back into the abdominal cavity, and mice were sutured and placed on a heating plate until recovery.

Retroviral Infections and Clonal Analyses

Retroviral infections were performed using a preparation of Moloney murine leukemia retrovirus expressing GFP under control of the CAG promoter (Jessberger et al., 2007). Lateral ventricles of E13.5 embryos were injected following the same protocol as for in utero electroporation. In utero infection of cortical progenitors was performed with a limiting dilution of GFP retrovirus in WT and KO mice at E13.5 (Jagasia et al., 2009). In these conditions, we consistently labeled a few isolated neurons and a couple of small groups of neurons, clearly isolated from each other (average number of cells per clones = 4.7; average number of clones per animal analyzed = 3.4; not found in the same section for instance or separated by at least 300 μm in depth). We focused our analysis on the isolated groups of radially oriented neurons in the somatosensory cortex that consisted of clonally related cells (Figure S4).

Organotypic Slice Culture and Time Lapse

Embryonic brains were electroporated at E14.5, and 300 μm embryonic brain slices were prepared at E15.5 using a Leica VT1000S vibrosector. Slices were cultured on confocal inserts (Millipore; 5 mm height) with 1.2 ml of Hank's balanced salt solution (HBSS) supplemented with Eagle's basal medium and 5% of horse serum (Invitrogen). Time lapse confocal microscopy was performed using an LD Plan Neofluar 20×/0,40 with a Zeiss LSM 510 inverted microscope by imaging multiple z stacks at preselected positions on a given set

of electroporated slices. Repetitive acquisitions were performed every 20 min for up to 20 hr, and movies were assembled with Zeiss Zen imaging software. Thirty neurons per slice were randomly selected within the SVZ/IZ and tracked using the Manual Tracking plugin of ImageJ software. The position of each individual neuron was manually marked as the center of the neuron and recorded as XY coordinate on each image of 1,024 × 1,024 pixels. The length of the migration between consecutive time frames was calculated by converting the length of the XY vector formed between to time frames in microns (1.024 pixels = 300 μm). Following ephrin-B1 overexpression, a neuron was considered as "clustered" if it belongs to a group of at least five cells in contact with each other and "single" if its position is more than 10 μm away from a cluster at the end of the time lapse acquisition. The parameters of migration were calculated using homemade calculation software and Microsoft Excel 2011.

Immunofluorescence

Embryos were fixed by transcardiac perfusion with 4% paraformaldehyde (Invitrogen). Brains were dissected, and 100 μm sections were prepared using a Leica VT1000S vibrosector. Slices were transferred into PBS/0.3% Triton X-100 (PBST), blocked with PBST/3% horse serum during 1 hr, and incubated overnight at 4°C with the following primary antibodies: chicken anti-GFP (Abcam, 1:2,000), mouse anti-Map2 (Sigma, 1:500), rabbit anti-Cux1 (Santa Cruz Biotechnology, 1:1,000), rat anti-Ctip2 (Abcam, 1:500), rat anti-BrdU (Abcam, 1:500), rabbit anti-Ki67 (Abcam, 1:500), rabbit anti-Nestin (Covance, 1:1,000), mouse anti-MYC (Cell Signaling, 1:500), rabbit anti-RFP (Abcam, 1:500), and mouse anti-Efb1-3 (Santa Cruz Biotechnology, 1:200). After three PBS washes, slices were incubated in PBS during 1 hr at room temperature and incubated 2 hr at room temperature with the secondary antibody: Alexa-488 goat anti-chicken (1:1,000, Molecular Probes) or Cyanine 3 donkey anti-rat, anti-mouse, or anti-rabbit (1:500, Jackson ImmunoResearch). Slices were then treated as described elsewhere (Dufour et al., 2003). Analyses were performed using a Zeiss Axioplan fluorescence microscope or a Zeiss LSM510 confocal microscope.

Immunohistochemistry

For immunohistochemistry, paraffin sections 4 μm thick were incubated at 98°C for 30 min in sodium citrate buffer (10 mM sodium citrate, 0.2% Tween 20, pH 6.0). The sections were immersed in 0.2% hydrogen peroxide for 30 min and preincubated in a humid chamber in PBS plus 5% horse serum with 0.3% Tween 20 for 30 min at room temperature, followed by overnight incubation with goat-ephrinB1 (1:40, R&D Systems) at 4°C. The sections were incubated with biotinylated rabbit anti-goat immunoglobulin G (5.0 mg/ml), followed by an avidin-biotin peroxidase complex, and developed by immersing in DAB substrate according to the manufacturer's instructions (Vectastain Elite ABC kit, Vector). The specificity of the staining was verified by incubation without the primary or secondary antibodies.

Constructs

Mouse ephrin-B1 complementary DNA (with or without Myc-tag sequence) was cloned into pCAG-IRES-GFP (pCIG) plasmid using XhoI/HindIII restriction sites. Ephrin-B1T was deleted for the last 72 amino acids, fused in frame with enhanced green fluorescent protein sequence, and cloned into pCAG-IRES-RFP plasmid using XhoI/HindIII restriction sites. pEGFP plasmids with GFP-tagged WT or dominant-negative human Prex1 and Myc-tagged WT or ΔPDZ human Prex1 are a kind gift of M. Hoshino (Kyoto University Graduate School of Medicine). N-terminal 3× Flag-tagged WT and dominant-negative (T17N) human Rac3 in pCDNA3.1 were a kind gift from J. Collard (The Netherlands Cancer Institute). They were amplified by PCR, sequence verified, and cloned into pCIG using XhoI and EcoRI restriction sites. B1S37 EfnB1 S37D (A358G) was generated by PCR from pCIG-EfnB1 (F primer: ctcga gatggcccggcctgggca; R primer: tttgaattccaggcccatgtagtCggggctgaactcttg), sequence verified, and cloned back into pCIG-EfnB1 with XhoI (within pCIG multiple cloning site) and EcoRI (within EfnB1 coding sequence).

Adhesion Assays

For adhesion assays, embryos were in utero electroporated with pCIG or pCIG-EfnB1 at E14.5 as described earlier. After 24 hr, embryos were removed and brains were dissected, after which the GFP-expressing regions were microdissected under a fluorescent binocular microscope in cold HBSS (Invitrogen, #14025). Tissue was rinsed three times in HBSS without Ca^{2+}/Mg^{2+} (Invitrogen, #14170), incubated for 15 min at 37°C in HBSS without Ca^{2+}/Mg^{2+} supplemented with 1 mM EDTA, and gently pipetted to obtain a single-cell suspension. Cells (1×10^5) were plated on coverslips coated with ephrin or Eph Fc fusion proteins and routinely cultured in Neurobasal (Invitrogen, 21103) supplemented with 1× N2 (Invitrogen, 17502), 1× B27 without VitA (Invitrogen, #12587), 2 mM L-glutamine (Invitrogen, #25030), and 50 U/ml penicillin/streptomycin (Invitrogen, #151070). After 1 hr and 24 hr, plates were gently tapped and rinsed with PBS, and cells were fixed in 4% paraformaldehyde for 30 min, washed three times in PBS, and then stained for GFP and Hoechst. At least 500 cells from 5 to 10 random fields per experiment and condition were counted by a blinded person, and the proportion of GFP+ cells among the total number of cells per field was calculated.

Immunoprecipitation and Western Blotting

Brains were in utero electroporated at E13.5 with the indicated plasmids. At E14.5, electroporated cortices (n = at least three per condition) were dissected in cold HBSS and lysed in NP40 buffer (containing 20 mM Tris-HCl at pH 8, 137 mM NaCl, 10% glycerol, 1% Igepal [NP-40], 2 mM EDTA). Extracts were cleared by centrifugation for 15 min at 4°C and precleared for 1 hr with protein A/G beads. Immunoprecipitation was performed with 2 μg of anti-ephrin-B1 (R&D Systems), anti-NeuroD1 (control antibody, Santa Cruz Biotechnology), or anti-MYC (Roche) overnight at 4°C, followed by incubation for 1 hr with protein A/G beads; washing and elution were performed according to standard protocols with NP40 buffer. Western blotting was performed according to standard protocols with antibodies recognizing ephrin-B1, GFP, Myc, and Actin.

SUPPLEMENTAL INFORMATION

Supplemental Information includes seven figures and two movies and can be found with this article online at http://dx.doi.org/10.1016/j.neuron.2013.07.015.

ACKNOWLEDGMENTS

We thank Gilbert Vassart for continuous support and interest; members of the lab and the Institut de Recherche en Biologie Humaine et Moléculaire for helpful discussions and advice; Dr. Bollet-Quivogne (Fonds de la Recherche Scientifique [FNRS] Logistic Scientist) of the Light Microscopy Facility for his support with imaging; Giuseppe Saldi for computation of the time-lapse analysis data set; and Viviane De Maertelaer and Jerome Bonnefont for advice on statistical analyses. We thank Dr. Hoshino and Dr. Collard for reagents to study P-Rex1 and Rac3. This work was funded by grants from the Belgian FNRS, Fonds pour la Recherche de l'Industrie et l'Agriculture, and Fonds pour la Recherche Scientifique Médicale; the Belgian Queen Elizabeth Medical Foundation; the Action de Recherches Concertées Programs; the Interuniversity Attraction Poles Program; the Belgian State; the Federal Office for Scientific, Technical and Cultural Affairs; the Welbio and Programme d'Excellence CIBLES of the Walloon Region; the Fondations Université Libre de Bruxelles; and Pierre Clerdent and Roger de Spoelberch (to P.V.). P.V. is research director, L.T. is a postdoctoral fellow, and J.V.D.A and L.P. are doctoral fellows of the FNRS.

Accepted: July 12, 2013
Published: September 18, 2013

REFERENCES

Arvanitis, D.N., Béhar, A., Tryoen-Tóth, P., Bush, J.O., Jungas, T., Vitale, N., and Davy, A. (2013). Ephrin B1 maintains apical adhesion of neural progenitors. Development *140*, 2082–2092.

Batlle, E., and Wilkinson, D.G. (2012). Molecular mechanisms of cell segregation and boundary formation in development and tumorigenesis. Cold Spring Harb. Perspect. Biol. *4*, a008227.

Bielas, S., Higginbotham, H., Koizumi, H., Tanaka, T., and Gleeson, J.G. (2004). Cortical neuronal migration mutants suggest separate but intersecting pathways. Annu. Rev. Cell Dev. Biol. *20*, 593–618.

Bochenek, M.L., Dickinson, S., Astin, J.W., Adams, R.H., and Nobes, C.D. (2010). Ephrin-B2 regulates endothelial cell morphology and motility independently of Eph-receptor binding. J. Cell Sci. *123*, 1235–1246.

Clandinin, T.R., and Feldheim, D.A. (2009). Making a visual map: mechanisms and molecules. Curr. Opin. Neurobiol. *19*, 174–180.

Compagni, A., Logan, M., Klein, R., and Adams, R.H. (2003). Control of skeletal patterning by ephrinB1-EphB interactions. Dev. Cell *5*, 217–230.

Cowan, C.A., and Henkemeyer, M. (2001). The SH2/SH3 adaptor Grb4 transduces B-ephrin reverse signals. Nature *413*, 174–179.

Dufour, A., Seibt, J., Passante, L., Depaepe, V., Ciossek, T., Frisén, J., Kullander, K., Flanagan, J.G., Polleux, F., and Vanderhaeghen, P. (2003). Area specificity and topography of thalamocortical projections are controlled by ephrin/Eph genes. Neuron *39*, 453–465.

Egea, J., and Klein, R. (2007). Bidirectional Eph-ephrin signaling during axon guidance. Trends Cell Biol. *17*, 230–238.

Flanagan, J.G., and Vanderhaeghen, P. (1998). The ephrins and Eph receptors in neural development. Annu. Rev. Neurosci. *21*, 309–345.

Friocourt, G., Kanatani, S., Tabata, H., Yozu, M., Takahashi, T., Antypa, M., Raguenes, O., Chelly, J., Ferec, C., Nakajima, K., and Parnavelas, J.G. (2008). Cell-autonomous roles of ARX in cell proliferation and neuronal migration during corticogenesis. J. Neurosci. *28*, 5794–5805.

Fuentes, P., Canovas, J., Berndt, F.A., Noctor, S.C., and Kukuljan, M. (2012). CoREST/LSD1 control the development of pyramidal cortical neurons. Cereb. Cortex *22*, 1431–1441.

Genander, M., and Frisén, J. (2010). Ephrins and Eph receptors in stem cells and cancer. Curr. Opin. Cell Biol. *22*, 611–616.

Guerrier, S., Coutinho-Budd, J., Sassa, T., Gresset, A., Jordan, N.V., Chen, K., Jin, W.L., Frost, A., and Polleux, F. (2009). The F-BAR domain of srGAP2 induces membrane protrusions required for neuronal migration and morphogenesis. Cell *138*, 990–1004.

Hajdo-Milasinović, A., Ellenbroek, S.I., van Es, S., van der Vaart, B., and Collard, J.G. (2007). Rac1 and Rac3 have opposing functions in cell adhesion and differentiation of neuronal cells. J. Cell Sci. *120*, 555–566.

Hajdo-Milasinović, A., van der Kammen, R.A., Moneva, Z., and Collard, J.G. (2009). Rac3 inhibits adhesion and differentiation of neuronal cells by modifying GIT1 downstream signaling. J. Cell Sci. *122*, 2127–2136.

Hand, R., Bortone, D., Mattar, P., Nguyen, L., Heng, J.I., Guerrier, S., Boutt, E., Peters, E., Barnes, A.P., Parras, C., et al. (2005). Phosphorylation of Neurogenin2 specifies the migration properties and the dendritic morphology of pyramidal neurons in the neocortex. Neuron *48*, 45–62.

Huynh-Do, U., Vindis, C., Liu, H., Cerretti, D.P., McGrew, J.T., Enriquez, M., Chen, J., and Daniel, T.O. (2002). Ephrin-B1 transduces signals to activate integrin-mediated migration, attachment and angiogenesis. J. Cell Sci. *115*, 3073–3081.

Ip, J.P.K., Shi, L., Chen, Y., Itoh, Y., Fu, W.-Y., Betz, A., Yung, W.-H., Gotoh, Y., Fu, A.K.Y., and Ip, N.Y. (2011). α2-chimaerin controls neuronal migration and functioning of the cerebral cortex through CRMP-2. Nat. Neurosci. *15*, 39–47.

Jagasia, R., Steib, K., Englberger, E., Herold, S., Faus-Kessler, T., Saxe, M., Gage, F.H., Song, H., and Lie, D.C. (2009). GABA-cAMP response element-binding protein signaling regulates maturation and survival of newly generated neurons in the adult hippocampus. J. Neurosci. *29*, 7966–7977.

Jessberger, S., Zhao, C., Toni, N., Clemenson, G.D., Jr., Li, Y., and Gage, F.H. (2007). Seizure-associated, aberrant neurogenesis in adult rats characterized with retrovirus-mediated cell labeling. J. Neurosci. *27*, 9400–9407.

Jørgensen, C., Sherman, A., Chen, G.I., Pasculescu, A., Poliakov, A., Hsiung, M., Larsen, B., Wilkinson, D.G., Linding, R., and Pawson, T. (2009). Cell-specific information processing in segregating populations of Eph receptor ephrin-expressing cells. Science *326*, 1502–1509.

Jossin, Y., and Cooper, J.A. (2011). Reelin, Rap1 and N-cadherin orient the migration of multipolar neurons in the developing neocortex. Nat. Neurosci. *14*, 697–703.

Klein, R. (2009). Bidirectional modulation of synaptic functions by Eph/ephrin signaling. Nat. Neurosci. *12*, 15–20.

Kriegstein, A.R., and Noctor, S.C. (2004). Patterns of neuronal migration in the embryonic cortex. Trends Neurosci. *27*, 392–399.

Kwiatkowski, A.V., Rubinson, D.A., Dent, E.W., Edward van Veen, J., Leslie, J.D., Zhang, J., Mebane, L.M., Philippar, U., Pinheiro, E.M., Burds, A.A., et al. (2007). Ena/VASP Is Required for neuritogenesis in the developing cortex. Neuron *56*, 441–455.

Lallemand, Y., Luria, V., Haffner-Krausz, R., and Lonai, P. (1998). Maternally expressed PGK-Cre transgene as a tool for early and uniform activation of the Cre site-specific recombinase. Transgenic Res. *7*, 105–112.

Li, Y., Lu, H., Cheng, P.L., Ge, S., Xu, H., Shi, S.H., and Dan, Y. (2012). Clonally related visual cortical neurons show similar stimulus feature selectivity. Nature *486*, 118–121.

LoTurco, J.J., and Bai, J. (2006). The multipolar stage and disruptions in neuronal migration. Trends Neurosci. *29*, 407–413.

Marín, O., and Rubenstein, J.L.R. (2003). Cell migration in the forebrain. Annu. Rev. Neurosci. *26*, 441–483.

Marín, O., Valiente, M., Ge, X., and Tsai, L.H. (2010). Guiding neuronal cell migrations. Cold Spring Harb. Perspect. Biol. *2*, a001834.

Noctor, S.C., Martínez-Cerdeño, V., Ivic, L., and Kriegstein, A.R. (2004). Cortical neurons arise in symmetric and asymmetric division zones and migrate through specific phases. Nat. Neurosci. *7*, 136–144.

North, H.A., Zhao, X., Kolk, S.M., Clifford, M.A., Ziskind, D.M., and Donoghue, M.J. (2009). Promotion of proliferation in the developing cerebral cortex by EphA4 forward signaling. Development *136*, 2467–2476.

Ohshima, T., Hirasawa, M., Tabata, H., Mutoh, T., Adachi, T., Suzuki, H., Saruta, K., Iwasato, T., Itohara, S., Hashimoto, M., et al. (2007). Cdk5 is required for multipolar-to-bipolar transition during radial neuronal migration and proper dendrite development of pyramidal neurons in the cerebral cortex. Development *134*, 2273–2282.

Ohtsuki, G., Nishiyama, M., Yoshida, T., Murakami, T., Histed, M., Lois, C., and Ohki, K. (2012). Similarity of visual selectivity among clonally related neurons in visual cortex. Neuron *75*, 65–72.

Pacary, E., Heng, J., Azzarelli, R., Riou, P., Castro, D., Lebel-Potter, M., Parras, C., Bell, D.M., Ridley, A.J., Parsons, M., and Guillemot, F. (2011). Proneural transcription factors regulate different steps of cortical neuron migration through Rnd-mediated inhibition of RhoA signaling. Neuron *69*, 1069–1084.

Pinheiro, E.M., Xie, Z., Norovich, A.L., Vidaki, M., Tsai, L.-H., and Gertler, F.B. (2011). Lpd depletion reveals that SRF specifies radial versus tangential migration of pyramidal neurons. Nat. Cell Biol. *13*, 989–995.

Qiu, R., Wang, X., Davy, A., Wu, C., Murai, K., Zhang, H., Flanagan, J.G., Soriano, P., and Lu, Q. (2008). Regulation of neural progenitor cell state by ephrin-B. J. Cell Biol. *181*, 973–983.

Rakic, P. (1988). Specification of cerebral cortical areas. Science *241*, 170–176.

Sentürk, A., Pfennig, S., Weiss, A., Burk, K., and Acker-Palmer, A. (2011). Ephrin Bs are essential components of the Reelin pathway to regulate neuronal migration. Nature *472*, 356–360.

Stuckmann, I., Weigmann, A., Shevchenko, A., Mann, M., and Huttner, W.B. (2001). Ephrin B1 is expressed on neuroepithelial cells in correlation with neocortical neurogenesis. J. Neurosci. *21*, 2726–2737.

Sun, Y., Fei, T., Yang, T., Zhang, F., Chen, Y.G., Li, H., and Xu, Z. (2010). The suppression of CRMP2 expression by bone morphogenetic protein (BMP)-SMAD gradient signaling controls multiple stages of neuronal development. J. Biol. Chem. *285*, 39039–39050.

Tabata, H., and Nakajima, K. (2003). Multipolar migration: the third mode of radial neuronal migration in the developing cerebral cortex. J. Neurosci. *23*, 9996–10001.

Tan, S.S., and Breen, S. (1993). Radial mosaicism and tangential cell dispersion both contribute to mouse neocortical development. Nature *362*, 638–640.

Torii, M., Hashimoto-Torii, K., Levitt, P., and Rakic, P. (2009). Integration of neuronal clones in the radial cortical columns by EphA and ephrin-A signalling. Nature *461*, 524–528.

Uchino, S., Hirasawa, T., Tabata, H., Gonda, Y., Waga, C., Ondo, Y., Nakajima, K., and Kohsaka, S. (2010). Inhibition of N-methyl-D-aspartate receptor activity resulted in aberrant neuronal migration caused by delayed morphological development in the mouse neocortex. Neuroscience *169*, 609–618.

Valiente, M., Ciceri, G., Rico, B., and Marín, O. (2011). Focal adhesion kinase modulates radial glia-dependent neuronal migration through connexin-26. J. Neurosci. *31*, 11678–11691.

Villar-Cerviño, V., Molano-Mazón, M., Catchpole, T., Valdeolmillos, M., Henkemeyer, M., Martínez, L.M., Borrell, V., and Marín, O. (2013). Contact repulsion controls the dispersion and final distribution of Cajal-Retzius cells. Neuron *77*, 457–471.

Waters, J.E., Astle, M.V., Ooms, L.M., Balamatsias, D., Gurung, R., and Mitchell, C.A. (2008). P-Rex1 - a multidomain protein that regulates neurite differentiation. J. Cell Sci. *121*, 2892–2903.

Westerlund, N., Zdrojewska, J., Padzik, A., Komulainen, E., Björkblom, B., Rannikko, E., Tararuk, T., Garcia-Frigola, C., Sandholm, J., Nguyen, L., et al. (2011). Phosphorylation of SCG10/stathmin-2 determines multipolar stage exit and neuronal migration rate. Nat. Neurosci. *14*, 305–313.

Xu, N.J., and Henkemeyer, M. (2009). Ephrin-B3 reverse signaling through Grb4 and cytoskeletal regulators mediates axon pruning. Nat. Neurosci. *12*, 268–276.

Xu, Z., Lai, K.-O., Zhou, H.-M., Lin, S.-C., and Ip, N.Y. (2003). Ephrin-B1 reverse signaling activates JNK through a novel mechanism that is independent of tyrosine phosphorylation. J. Biol. Chem. *278*, 24767–24775.

Yoshizawa, M., Kawauchi, T., Sone, M., Nishimura, Y.V., Terao, M., Chihama, K., Nabeshima, Y., and Hoshino, M. (2005). Involvement of a Rac activator, P-Rex1, in neurotrophin-derived signaling and neuronal migration. J. Neurosci. *25*, 4406–4419.

Yu, Y.C., Bultje, R.S., Wang, X., and Shi, S.H. (2009). Specific synapses develop preferentially among sister excitatory neurons in the neocortex. Nature *458*, 501–504.

Yu, Y.C., He, S., Chen, S., Fu, Y., Brown, K.N., Yao, X.H., Ma, J., Gao, K.P., Sosinsky, G.E., Huang, K., and Shi, S.H. (2012). Preferential electrical coupling regulates neocortical lineage-dependent microcircuit assembly. Nature *486*, 113–117.